Materials Science & Engineering C 100 (2019) 798–808

Contents lists available at ScienceDirect

Materials Science & Engineering C

journal homepage: www.elsevier.com/locate/msec

Encapsulated melatonin in polycaprolactone (PCL) microparticles as a promising graft material

Esra Bihter Gurler[a], Necdet Mekki Ergul[b,c], Burak Ozbek[b,c], Nazmi Ekren[d,c], Faik Nuzhet Oktar[e,c], Merve Erginer Haskoylu[e], Ebru Toksoy Oner[e], Mehmet Sayıp Eroglu[f], Dilek Ozbeyli[g], Veysel Korkut[h], Ahmet Furkan Temiz[h], Nil Kocanalı[h], Rosa Juvan Gungordu[h], Duhan Berkan Kılıckan[i], Oguzhan Gunduz[j,c,*]

[a] Department of Physiology, School of Medicine, Bahcesehir University, Istanbul, Turkey
[b] Department of Metallurgical and Materials Engineering, Institute of Pure and Applied Sciences, Marmara University, Istanbul 34722, Turkey
[c] Center for Nanotechnology&Biomaterials Application and Research at Marmara University, 34722, Goztepe Campus Istanbul, Turkey
[d] Department of Electrical and Electronics Engineering, Faculty of Technology, Marmara University, 34722 Istanbul, Turkey
[e] Department of Bioengineering, Faculty of Engineering, Marmara University, 34722 Istanbul, Turkey
[f] Department of Chemical Engineering, Faculty of Engineering, Marmara University, 34722 Istanbul, Turkey
[g] Department of Medical Pathological Techniques, Vocational School of Health Services, Marmara University, 34668 Istanbul, Turkey
[h] School of Medicine, Bahcesehir University, 34734 Istanbul, Turkey
[i] School of Medicine, Acıbadem University, 34752 Istanbul, Turkey
[j] Department of Metallurgical and Materials Engineering, Faculty of Technology, Marmara University, 34722 Istanbul, Turkey

ARTICLE INFO

Keywords:
Melatonin
Biodegradable polymer
Electrospraying
Graft

ABSTRACT

Electrospraying assures many advantages with taking less time and costing less relatively to the other conventional particle production methods. In this research, we investigated the encapsulation of melatonin (MEL) hormone in polycaprolactone (PCL) microparticles by using electrospraying method. Morphology analysis of the produced particles completed with Scanning Electron Microscopy (SEM). SEM images demonstrated that microparticles of 3 wt% PCL solution has the most suitable particle diameter size (2.3 ± 0.64 μm) for melatonin encapsulation. According to the characterization of the particles, electrospraying parameters like optimal collecting distance, the flow rate of the solution and voltage of the system detected as 8 cm, 0.5 ml/h, and 10 kV respectively. For determining the chemical bonds of scaffold Fourier-Transform Infrared Spectroscopy (FTIR) were used and FTIR results showed that melatonin successfully loaded into PCL micro-particles. Drug release kinetics of the melatonin loaded particles indicated that melatonin released with a burst at the beginning and release behavior became sustainable over a period of 8 h with the encapsulation efficiency of about 73%. In addition, both *in-vitro* and *in-vivo* studies of the graft materials also completed. Primary human osteoblasts (HOB) cells and female Sprague Dawley rats were used in *in-vitro* and *in-vivo* studies. Test results demonstrate cell population, and bone volume of the rats grafted with composites has remarkably increased, this caused remodelling in bone structure. Overall, these findings indicate that encapsulation of melatonin in the PCL particles with electrospray method is optimum for new synthetic graft material.

1. Introduction

Bone grafting is a surgical procedure, which restores bone with a material. According to their origins, they categorized as autogenous, allogenous, xenogenous, artificial or synthetic ones [1]. Even the gold standard is autogenous grafts; it is not always possible to obtain enough material *via* the patient's own body. On the other hand, increasing the cost of natural-origin grafts makes the synthetics and artificial grafts more popular.

In recent years, the biomedical industry gravitates towards to control drug delivery systems with the developed manufacturing technologies. These technologies enable to produce biocompatible and biodegradable micro and nano-sized particles contain different therapeutic agents, which released in particular amounts of time [2]. The reason for using this method is to overcome the low efficiency of delivery of drugs in a blasting cap, which can cause denaturation in the *in vivo*

* Corresponding author at: Center for Nanotechnology&Biomaterials Application and Research at Marmara University, 34722, Goztepe Campus, Istanbul, Turkey.
E-mail address: ucemogu@ucl.ac.uk (O. Gunduz).

https://doi.org/10.1016/j.msec.2019.03.051
Received 24 September 2018; Received in revised form 15 February 2019; Accepted 15 March 2019
Available online 16 March 2019
0928-4931/ © 2019 Elsevier B.V. All rights reserved.

environment [3]. Scientific studies indicated that polymeric particles could be very useful for biomedical applications. These particles mostly used as a drug delivery system, which can control the delivery of therapeutic agents. Changing the physical properties of the polymeric particle can affect the control mechanism of the drug delivery systems. Methods for producing these materials include solvent extraction/evaporation, spray drying, and suspension/emulsion polymerization. However, these conventional methods have some handicaps, such as polydispersity in particle size and low drug loading efficiency [4]. Recently, electrospraying technique came forward as an excellent alternative method for manufacturing these particles, because of the ability to produce near-monodisperse particles with size controlled by changing parameters of the process. In addition, this technique is much easier, faster and more economical when compared with other particle producing methods. [5].

Electrospraying systems are based on the dynamics of electrically charged fluids. The basic principle behind the electrospraying system is making much smaller particles by charging droplets coming out from the needle tip. Electrical forces overcome the force of surface tension in the charged polymeric solution. This led to Coulomb fission of droplets, which ends up with smaller jets [5,6].

Melatonin (*N*-acetyl-5-methoxytryptamine) (MEL) is a hormone, which produced majorly by the pineal gland in the brain. Melatonin hormone contributes to many physiological functions just like the regulation of circadian rhythms, immunomodulation, and reproduction. Recently, the investigations of melatonin's potential benefits show very promising results with bone-related disorders. According to these studies, melatonin inhibits osteoclast formation and osteoclastic activity *via* its free radical scavenging and anti-inflammatory actions [7,8].

Polycaprolactone (PCL) is widely used in tissue engineering operations because of their coherent physical properties. Polymeric scaffolds are the optimal environment for supporting mechanically robust, cell growth and undergo controlled biodegradation. PCL is exceptionally cheap biomaterial when compared with other biodegradable polymers and it has a slow degradation rate, and desirable mechanical properties [9]. The reason for using PCL instead of ceramics is obtaining better results for sustained releasing scaffolds. Polymeric materials are much more comprehensive due to growth factors, minerals, cells, and ions, which would improve and expedite functional bone or cartilage structure.

There is a lot of research in the literature relevant to the effects of many key variables of electrospraying. In these studies, Poly Lactic-co-Glycolic Acid (PLGA) is the most studied polymer and most preferred biodegradable polymer [10]. Nevertheless, in the present case of drug delivery for orthopedic applications, a slower degrading polymer like PCL is used. PCL is the Food and Drug Administration (FDA) approved and very suitable for encapsulating the drug in micro and nanoparticles. Also, it is very permeable to small drug molecules [11,12]. During the degradation, PCL offers lesser acidic environment [11]. Even so, there are very few studies about the fabrication of electrosprayed PCL particles in the recent literature [13,14]. PCL gave different characteristics to electrosprayed particles due to the complexity and interrelated of every unit relevant to the process [15].

The purpose of this study was to examine bone regeneration nature of encapsulated melatonin in PCL.

2. Materials and methods

2.1. Materials

Polycaprolactone (PCL, Mw = 80.000 g/mol) and melatonin powder (≥98% TLC) were obtained from Sigma-Aldrich (Munich, Germany). Dichloromethane (DCM) purchased from Merck (Darmstadt, Germany).

2.2. Preparation of PCL/melatonin solutions

PCL was dissolved with various percentages of 1, 3, 5 and 7 wt% in DCM. Solutions had stirred with the magnetic stirrer at ambient temperature (23 °C) for 1 h. After that step, 1.74 mg MEL was added separately in 3 wt% PCL solution and mixed with the magnetic stirrer for 1 h. 3 wt% PCL solution was selected because it is composing optimal properties for electrospraying.

2.3. Characterization of solutions

Characterizations of solutions performed by testing viscosity, electrical conductivity and density of the PCL solutions (1, 3, 5, and 7 wt%) at room temperature (25 °C). Viscosity was determined with a Brookfield DV-E Viscometer (Brookfield Instruments, Massachusetts, USA). Electrical conductivity measured using a Cond 3110 Set 1-2CA101 (WTW, Weilheim in Oberbayern, Germany). Density values obtained by a standard density bottle DIN ISO 3507-Gay-Lussac (Boru Cam, Istanbul, Turkey).

2.4. Preparation of melatonin loaded PCL microparticles

Microparticles fabricated using a Basic System (Inovenso, Turkey) electrospraying process (Fig. 1). As previously described, Taylor jet could be seen in Fig. 1a. First, 12 ml of the prepared polycaprolactone + melatonin (PCL + MEL) solution has pulled into 20 ml plastic syringe. Following the experimental conditions used for electrospray process: Flow rate applied by the syringe pump (IPS-12, Inovenso, Turkey) was 0.5 ml/h and solution pumped to the needle, which has 0.82 mm outer diameter and 0.51 mm inner diameter (Fig. 1a). Applied voltages changed between 10 and 15 kV. Collector covered with baking paper adjusted at 8 cm away from the needle. The experiment performed in 8 h. Following that, MEL loaded PCL particles peeled from baking paper carefully for further characterization tests.

2.5. Scanning electron microscopy (SEM) and optical microscopy

Morphology characterization of microparticles were fulfilled by using a scanning electron microscope (SEM) (EVO® LS 10, ZEISS, Germany) and optical microscope (BX51M, OLYMPUS, Japan) SEM applied with an accelerating voltage of 10 kV and surfaces of the prepared samples were coated with gold and palladium by using sputter (SC7620 Mini Sputter Coater, QUANTUM, United Kingdom) at 3 kV for 60 s. For investigation of particles diameter distribution, obtained SEM images of the particles analysed by using image software (Olympus AnalySIS, USA) and converted to excel data.

2.6. Thermal properties of the microparticles

Differential scanning calorimetry (DSC) used to determine the intermolecular interaction between components and extent of compatibility of melatonin with PCL core and the PCL fiber-shell. The peak values of endotherms taken as the melting temperature of the samples. Measurements performed using a Perkin Elmer Jade DSC instrument at a heating rate of 10 °C/min under the dynamic argon atmosphere (200 ml/min). The data was evaluated using Pyris software. Temperature and enthalpy calibration of the instrument performed periodically according to melting point and melting enthalpy of indium and zinc.

2.7. Fourier transform infrared spectroscopy (FTIR)

Fourier transform infrared (FTIR) spectroscopy (Jasco 4700 Spectrometer, Easton, USA) used to determine any chemical interaction between the polymers. The spectra recorded in the range of 400–4000 cm^{-1} under ambient temperature (23 °C). The system

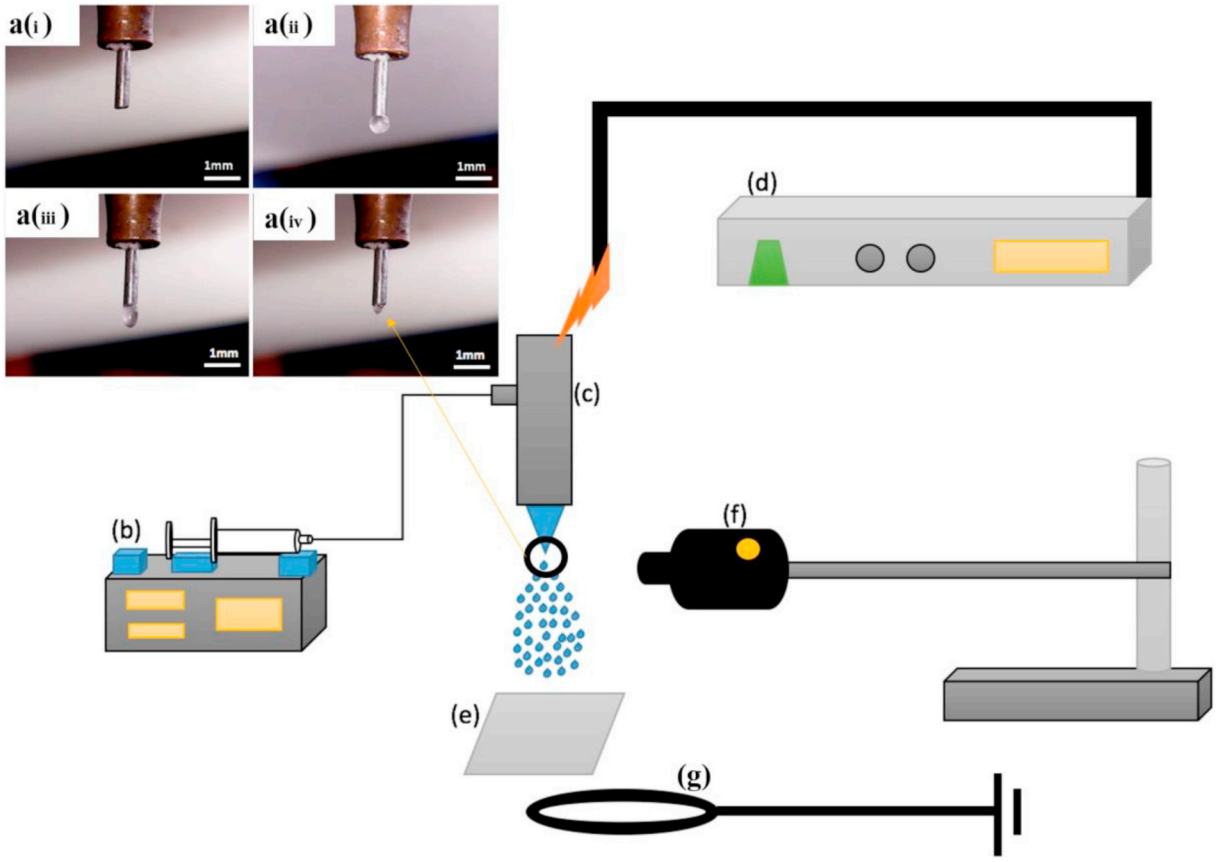


Fig. 1. (a) Close-up image of the atomization process (stable cone-jet mode) and Schematic of electrospray set-up, (b) syringe pump, (c) needle, (d) power supply, (e) collector, (f) camera.

aligned before data collection. Samples with different percentage of PCL and MEL loaded PCL were prepared and collected for analysis of FTIR.

2.8. Encapsulation efficiency and drug loading

UV–Vis Absorption Spectra completed by using a UV spectra machine (UV-1280, SHIMADZU, JAPAN). Prepared particles were loaded with MEL dropped into a phosphate buffer solution (PBS) with a 7.4 pH. The specific amount of particle/PBS solution (3 mg/ml) centrifuged for 8 h in total. Centrifuge process stopped in certain periods (15, 30, 45, 60, 120, 240, 300, 360, 420, and 480 min). After each period, the supernatant taken for UV absorption spectra. For each experiment, PBS changed with the fresh one. The encapsulation efficiency and drug loading calculated using the following relations. The melatonin loading in the PCL particles calculated based on Eq. (1). In addition, the drug-loading rate calculated by using Eq. (2).

$$\text{Encapsulation Efficiency (\%)} = \frac{\text{total concentration of drug} - \text{concentration of free drug}}{\text{total concentration of drug}} \times 100 \quad (1)$$

$$\text{Drug Loading} = \frac{\text{weight of MEL in PCL particles}}{\text{total weight of PCL particles}} \times 100 \quad (2)$$

2.9. In vitro studies

2.9.1. In vitro biocompatibility assay

To assess the biocompatibility of PCL and MEL loaded PCL microparticle cell proliferation and viability assay were completed. WST-1 (4-[3-(4-iodophenyl)-2-(4-nitrophenyl)-2H-5-tetrazolio]-1,3-benzenedisulfonate) (Roche Applied Science, Germany), was performed with a human osteoblast cell line (HOB). Electrosprayed PCL and MEL loaded microparticles had presterilized with 30 min UV both side, were followed by 70% ethanol sterilization for 30 min. and were set in 2% penicillin streptomycin in PBS for 2 h. After sterilization, scaffolds pre-saturated with Dulbecco's Modified Eagle Medium (DMEM) and this process lasted (10% FBS and 1% penicillin streptomycin) 2 h. Briefly, cells at the 70% confluency trypsinized seeded on to pre-sterilized and saturated scaffolds containing 24 well plates at the density of 1×10^4 and incubated for 24 and 72 h at 37 °C in humidified air, which were containing 5% CO_2. At the end of incubation period WST-1 reagent was added onto wells and was incubated for 2 h at dark 37 °C in 5% CO_2 and absorbance was measured at 405 nm by GloMax Multi + Microplate Multimode Reader (Promega, USA) untreated cells (cells on wells without any scaffold) were used as control and considered as 100% viable.

2.9.2. Cell behavior on electrosprayed scaffolds

Growth and attachment of HOB cells on electrosprayed scaffolds further investigated with fluorescence microscopy and SEM images. For this, scaffolds were incubated with cells for 24 and 72 h were fixed with 4% paraformaldehyde (PFA) in PBS solution and were washed with 1 × PBS 2 times. For Fluorescence microscopy nuclei of the cells are stained with DAPI (4′,6-diamidino-2-phenylindole, AppliChem, Germany) in the dark. After fixation and dying (scaffolds for fluorescence microscopy) both samples were dehydrated *via* rinsing in increasing ethanol concentrations (70, 80, 90, and 100%) and air-dried before further investigations with SEM and fluorescence microscopy.

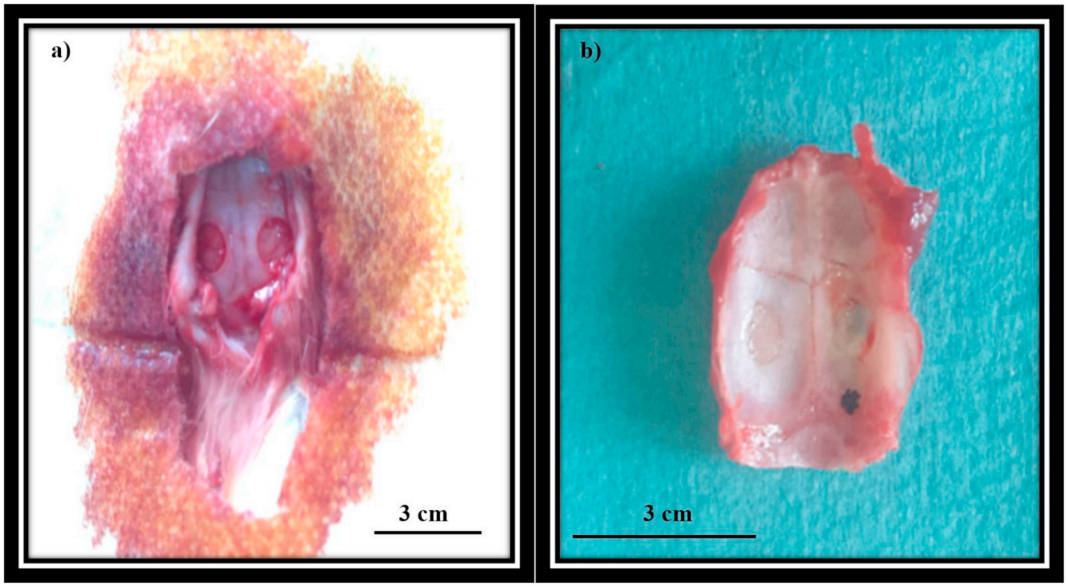


Fig. 2. (a) Rat calvarium showing 3 mm sized defect in parietal bone, (b) Representative image of harvested rat calvaria (black point shows control).

2.10. In vivo studies

2.10.1. Animals

Female Sprague Dawley rats (6–10 months old), were obtained from the Marmara University (MU) Animal Center (DEHAMER), kept under controlled conditions of humidity (65–70%) and temperature (22 ± 2 °C) and a standard light/dark (12 h/12 h) cycles. Rats had fed with standard rat pellets and water *ad libitum*. In compliance with the Turkish law on the use of animals in experiments, all experimental protocols approved by the MU Animal Care and Use Committee, and the principles and guidelines developed by the New York Academy of Sciences followed.

2.10.2. Surgery and the experimental groups

Under ketamine and chlorpromazine anesthesia (100 mg/kg and 0.75 mg/kg), a 3 cm midline incision was made on the skull and soft tissue was elevated. Under saline irrigation, a 3 mm defect bilaterally created on the cranium with a trephine drill (Fig. 2a.). Then the defects were either left empty (Control group; $n = 6$) or filled with PCL + MEL (Experimental group; $n = 6$). Skin incisions sutured, and the rats were returned to their cages. Animals sacrificed at 4th week after implantation.

2.10.3. Histomorphometry

At the end of the sacrification defect sites with surrounding bone were harvested (Fig. 2b). The cranial bones fixed in 10% formalin and transported to Erciyes University, Faculty of Dentistry Research Laboratory. The bones scanned using a micro-CT system (Skyscan 1172, Bruker, Belgium). Imaging was performed in the rotational plane at 116 μA, 86 kV for 60 min (camera pixel size: 4 μm). Reconstruction had carried outperforming a modified algorithm [16].

2.11. Statistical analysis

All statistical analysis performed with Graph Pad V 5.0 prims analysis program. Two-Way ANOVA followed by *post hoc* Tukey was performed for *in vitro* studies. Analysis of different groups in *in vivo* studies performed using unpaired Student's *t*-test was followed by Mann-Whitney with Graph Pad Prism 7.0 software. All experiments performed in triplicate and data were presented as mean and 95% confidence interval (CI). Differences were considered significant if $P < 0.05$. Values expressed as mean ± S.E.M.

3. Results

3.1. Particle morphology

Figs. 3 and 4 indicated particle size and morphology, both of them affected by the change in polymer concentration. Particle size revealed variability between 9.13 ± 2.36 μm and 2.30 ± 0.64 μm by decreasing flow rate from 1.5 ml/h to 0.5 ml/h. The diameter of microparticles was between 2.30 and 9.13 μm and these were depending on the electrospray solutions and parameters. 3 wt% PCL solution was obtained the best shape and diameter when compared to the others (Fig. 4d).

3.2. Thermal behavior

The DSC curves of pure MEL and PCL + MEL microspheres collectively given in Fig. 5a and b respectively.

3.3. FTIR analysis

In order to detect the molecular arrangement of PCL + MEL microparticles, FTIR analysis fulfilled. Fig. 5c proved the FTIR spectra of the microparticles. There was a typical PCL related infrared band stretching was detected.

3.4. Encapsulation efficiency of melatonin loaded PCL microparticles

1.74 mg of MEL loaded microparticles dispersed in PBS buffer solution (pH 7.4) for 8 h in total. The amount of released drug observed by using UV Spectrophotometer (UV-1280, SHIMADZU, JAPAN). Furthermore, drug loading of the particles has found 58% for the 1.74 mg of MEL used. Fig. 6c indicated a release profile of the melatonin loaded PCL microparticles. The Higuchi and Korsmeyer-Papas models used for the final particle formulation. The Higuchi model indicated using Eq. (3) [17].

$$Mt = k_H \sqrt{t} \quad (3)$$

In this equation, M_t is the quantity of cumulative drug released at time t, and kH is the Higuchi constant. From this equation, Higuchi model calculated as 0.84697 which was indicated non-Fickian mechanisms. Korsmeyer-Peppas model applied to search circumstantial mechanisms from the polymeric matrix and indicated by using Eq. (4)

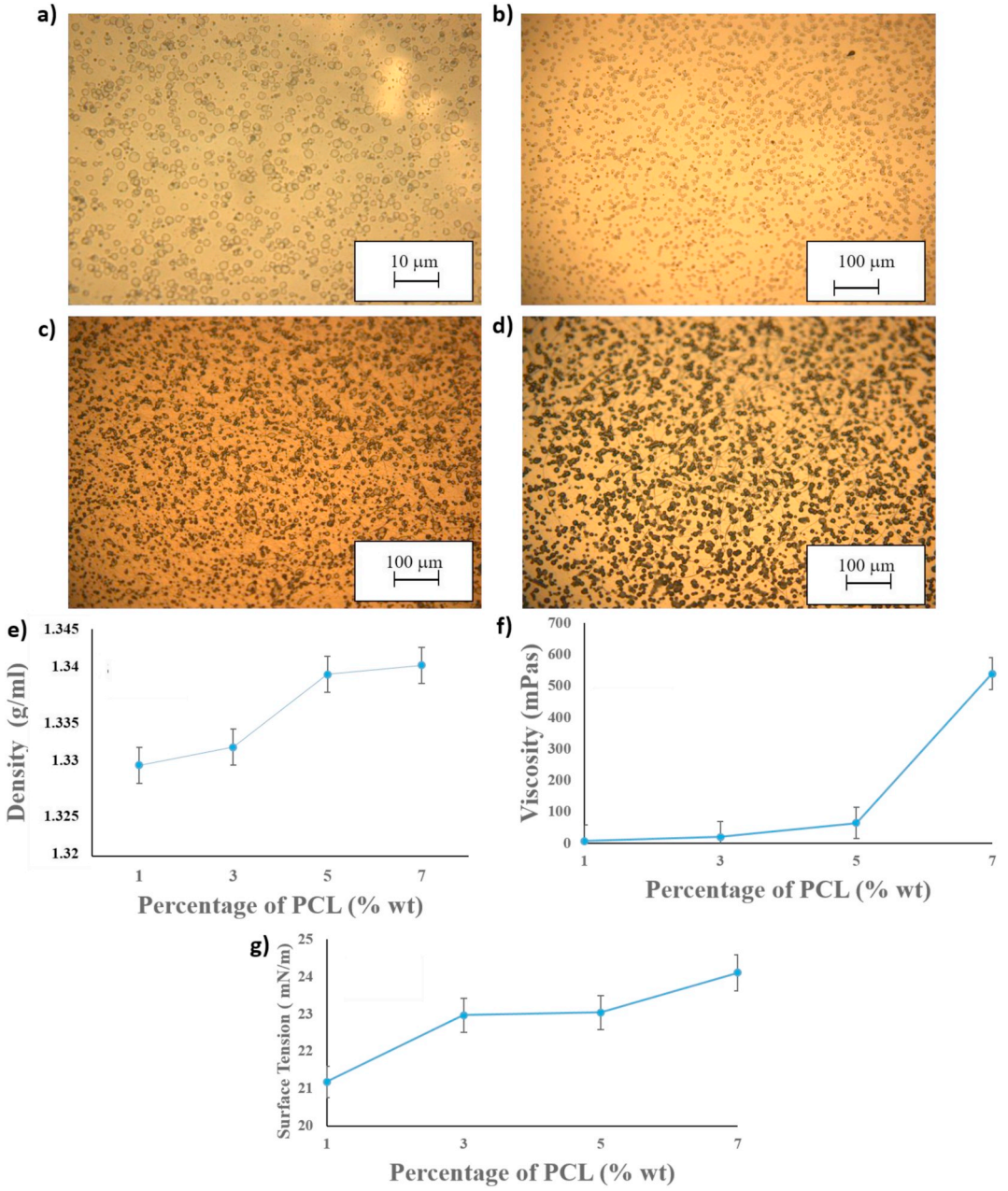


Fig. 3. Optical microscopy images of PCL microparticles and physical properties of the PCL solutions (a) 1 wt% PCL microparticles, (b) 3 wt% PCL microparticles, (c) 5 wt% PCL microparticles, (d) 7 wt% PCL microparticles, (e) density, viscosity and surface tension of the solutions.

[17].

$$\frac{M_t}{M_\infty} = k\, t^n \tag{4}$$

In this equation Mt / M∞ is the ratio of melatonin released at time, t. k is the release rate constant and n is the release exponent. This equation describes the mechanism of drug release. The release exponent can found with Eq. (5) [17].

$$\log\left(\frac{Mt}{M\infty} \times 100\right) = n\, logt \times \log k \tag{5}$$

3.5. In vitro results

Proliferation and Cell Viability of HOB cells on electrosprayed scaffolds were investigated for 24 and 72 h. Whereas viability of PCL and PCL + MEL samples were 93.02% and 95.30% at the day 1 (Fig. 7c), and viabilities had changed to 95.19% and 101.9% at the day 3 (Fig. 7c.). In addition, the SEM image of the MEL loaded PCL particles could be seen in Fig. 7e.

Cell behavior on PCL and PCL + MEL samples were observed *via* fluorescent microscopy (Leica DM LB2, Leica Microsystems, Wetzlar, Germany) and images were captured with IM50. DAPI stained cell nuclei after 24 h and 72 h incubation with scaffolds were indicated in Fig. 7. Cells were indicated in control, which had seeded on to glass. It clearly indicated in the images (Fig. 7a and b) that cells attached to samples and cell population increased with time.

Oneway Anova and Tukey analysis of control, PCL and PLC-MEL samples had indicated no significance at the 24th h ($P > 0.05$). Same tests had shown significance at 72th h for those control-PCL and control-PCL + MEL ($P > 0.05$), while no significance observed between PCL and PCL + MEL ($P > 0.05$).

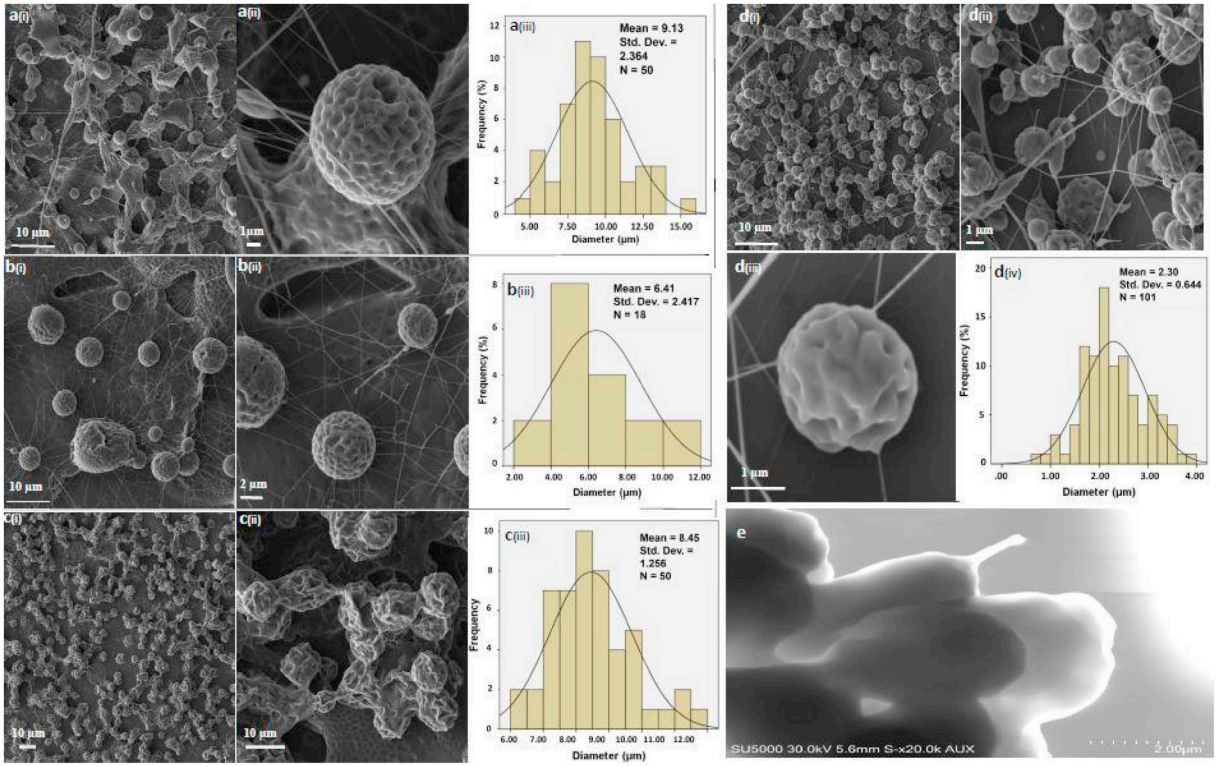


Fig. 4. SEM images of PCL microparticles produced at different polymer concentration and SEM, TEM images of the 3 wt% PCL particle and size distribution of it (a) 7 wt% PCL-DCM, (b) 5 wt% PCL-DCM, (c) 1 wt% PCL-DCM, and (d) SEM image of the microparticle and size distribution (e) TEM image of the PCL + MEL microspheres.

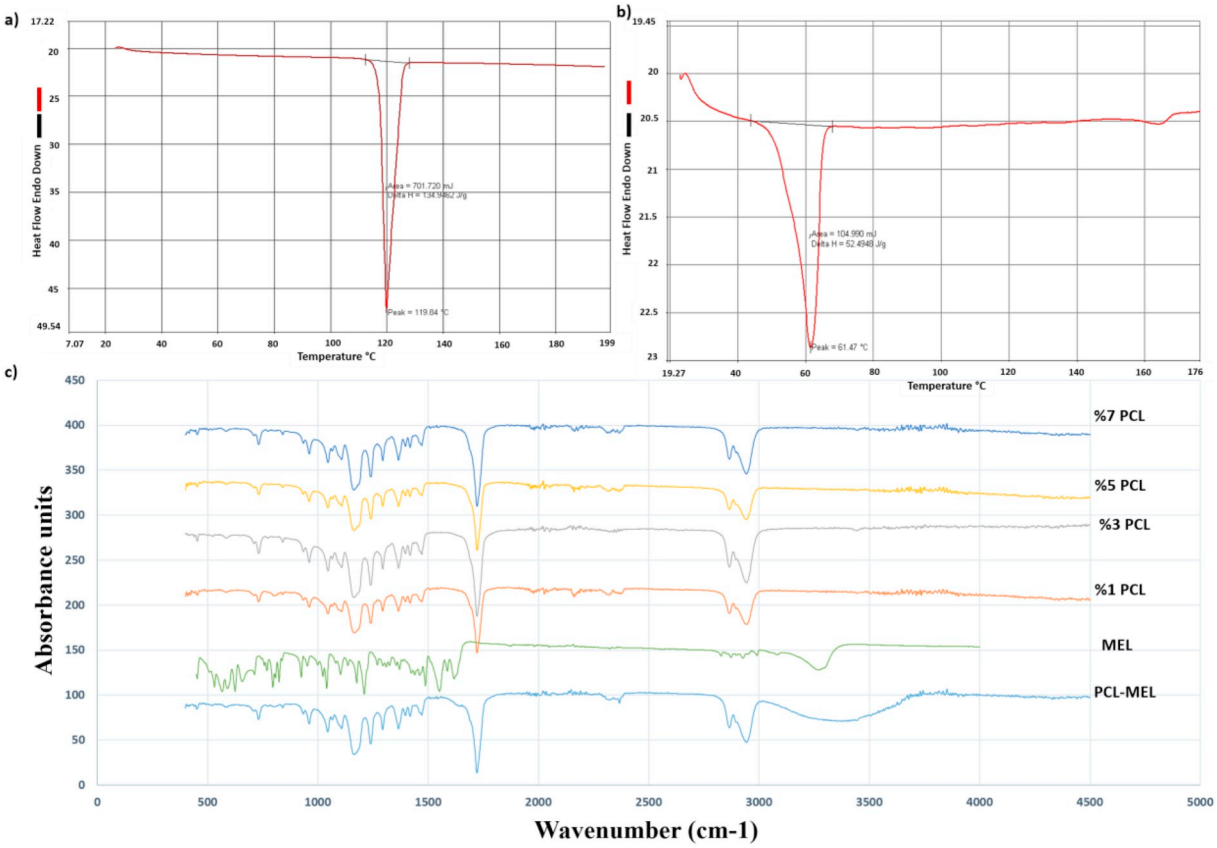


Fig. 5. DSC curves and FTIR spectra of the samples (a) DSC curve of melatonin, (b) DSC curve of melatonin encapsulated in PCL, (c) FTIR spectra of the 1, 3, 5, and 7 wt% PCL and melatonin loaded PCL particles between 400 and 4000 cm^{-1} wavelengths.

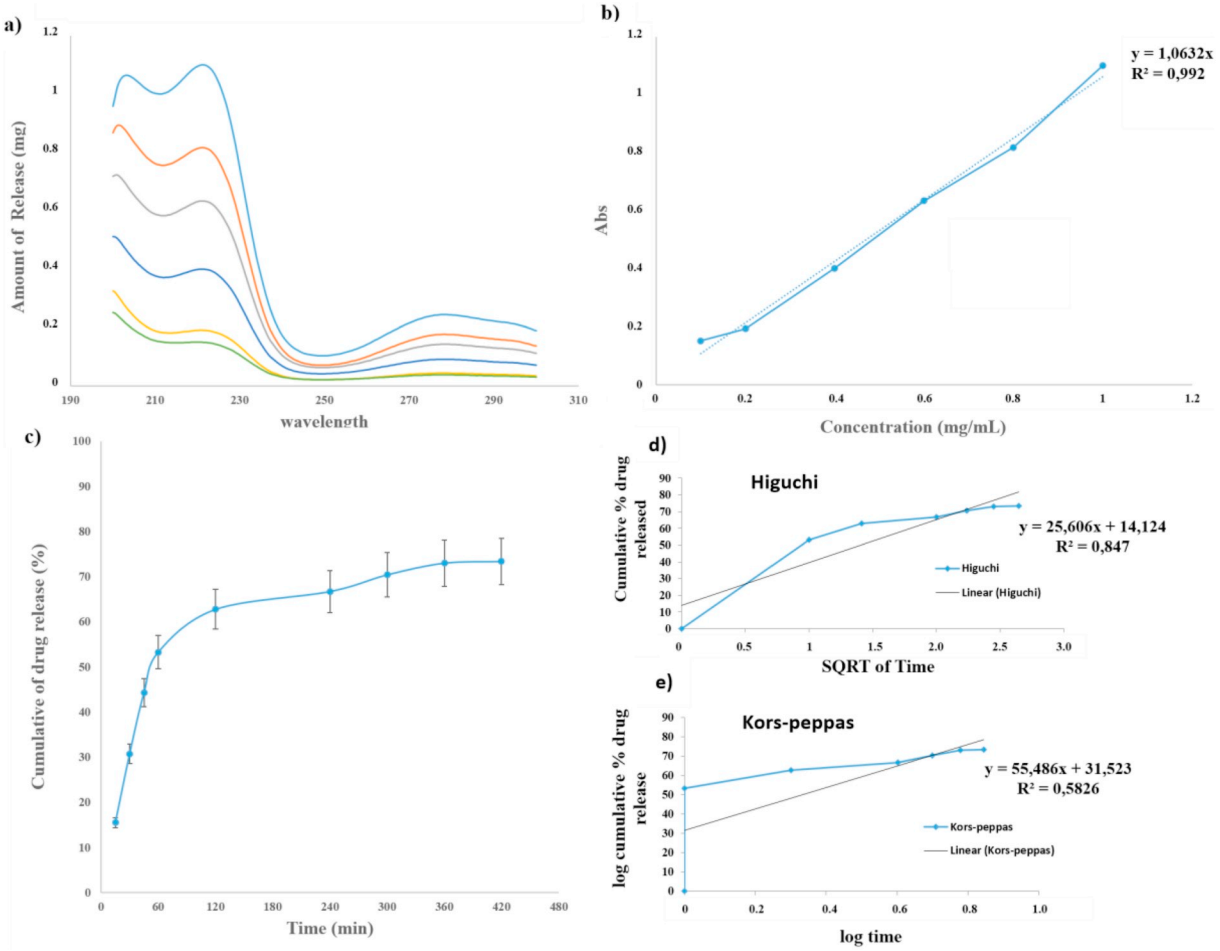


Fig. 6. Drug release profile of the melatonin loaded PCL microparticles (a) amount of release drug by time in PBS, (b) calibration curve of melatonin, (c) drug release efficiency of particles, (d) Higuchi model and Korsmeyer-Peppas model of drug release.

3.6. In vivo studies

Bone volume and bone surface area/total surface area were measured histomorphometrically (Fig. 8.). When examined at the 4th week of surgery, the bone volume of rats was grafted with PCL + MEL was significantly ($P < 0.05$) elevated with respect to that of the control group (Fig. 8b.). Additionally, graft resorption did not observe macroscopically in any of the PCL + MEL subjects. In accordance with the bone volume results, bone surface area / total surface area ratio was greater in the polycaprolactone + melatonin (PCL + MEL) group (Fig. 8c.).

4. Discussion

It has discovered that the decrease in polymer concentration had caused smaller particle diameter formation. By changing polymer concentration between 7 and 1 wt%, smoother particles could be produced. It also understood that particle size was affected by the different flow rate of the polymer solution, which was pumped through the syringe pump [18]. Regular size of human capillaries is about 8 μm, for this reason, particles size should be < 8 μm for intravenous injection [19]. It is not possible to fabricate spherical particles from a high concentration PCL solution by electrospraying, which can be seen in Fig. 3b. It's still not possible when reducing the solution concentration to 10 wt%, and this condition is led to smooth PCL fibers, not particles.

When the concentration of PCL was decreased from 5 to 7 to 1–3 wt % very fine PCL microparticles produced instead of PCL fibers. Polymer concentration was affected most of the physical properties of PCL. Density, viscosity and surface tension were increased, when PCL concentration had increased from 1 to 7 wt% (Fig. 3). Nevertheless, electrical conductivity is always zero in PCL-DCM solution [20]. All of the experimental conditions were given in Table 1. Applied voltage also controls as a parameter to control the morphology of electrosprayed particles. The common opinion is increasing the applied voltage cause a decrease in the size of micro-particles. However, there are some lower and upper voltage limits allow a stable jet in electrospraying. For the solutions with 1 and 3 wt% PCL concentrations, the lower voltage applied for producing more uniform PCL particles (Fig. 4) [21].

A remarkable endothermic peak was observed at 119 °C, which is due to the melting of melatonin, indicating its crystalline structure (Fig. 5a). The melting endotherms were observed nearly at 61 °C due to the melting of PCL, respectively, which are inherently crystalline polymers. This curve has no melting endotherm corresponding to melatonin melting temperature shown in Fig. 5a. This indicates that a fully amorphous and uniform distribution of melatonin in hydrophobic PCL core was presented. It was notable that the homogenous distribution of melatonin in the PCL core provides a significant advantage in the controlled and sustainable release.

Also, this application tended to produce smaller particles (Fig. 4). The stronger electric field at higher voltages forces the conical meniscus at the needle and this cause breaking smaller droplets as indicated in Fig. 3. [22]. The TEM image was given in Fig. 4e had displayed a uniform morphology of the melatonin-loaded spherical PCL core in the inner layer, which was darker than the outer layer. A more homogeneous layer with light color was indicating a shell, which completely was covering the PCL microparticles.

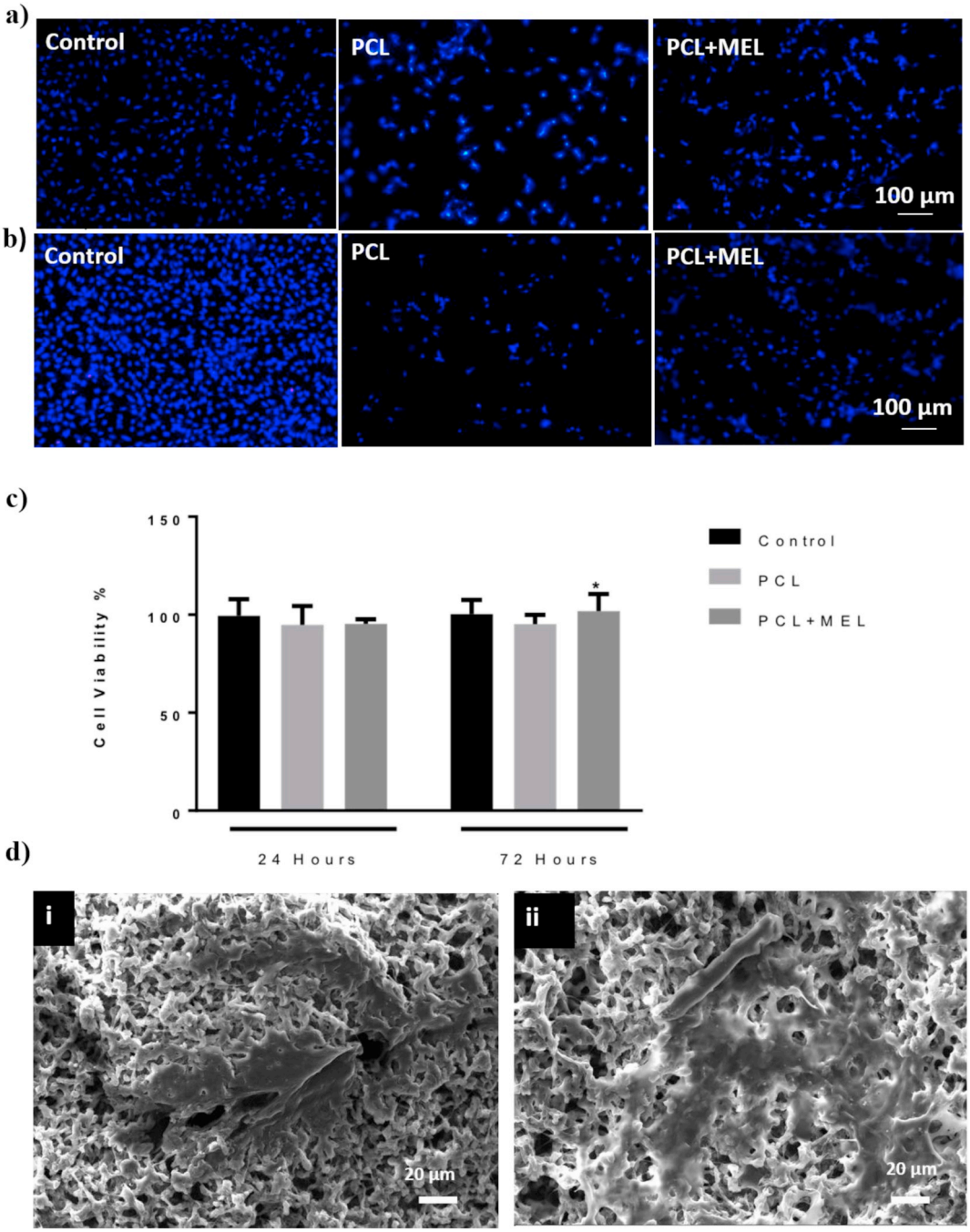


Fig. 7. Fluorescent microscopy images of HOB cell post culture, HOB cell viability results after cultivation with PCL, PCL + Mel electrosprayed scaffold and SEM image of melatonin loaded PCL particles after cell proliferation (a) Fluorescent microscopy image of 24 h HOB cell post culture, (b) Fluorescent microscopy image of 72 h HOB cell post culture, (c) HOB cell viability results of 24 h cell cultured particles, HOB cell viability results of 72 h cell cultured particles, (d) SEM image of 24 h and 72 h cell cultured PCL + MEL particles.

FTIR results had indicated an asymmetric CH2 stretching peak at 2949 cm^{-1}, symmetric CH2 stretching peak at 2850 cm^{-1}, carbonyl stretching peak at 1720 cm^{-1}, C—O and C—C stretching peak at 1285 cm^{-1} and asymmetric COC stretching peak at 1240 cm^{-1} were observed [20]. The FTIR spectrum of melatonin stretching peaks were determined at 3333.59 cm^{-1} 1625 cm^{-1} and 1210 cm^{-1} associated with the functional N—H stretch, C═O and C—N respectively [23]. The FTIR spectra of particles have proved in Fig. 5c. It is shown that PCL-related stretching modes were consisting of every microparticle sample including melatonin extract with compering with lower peak strengths [24]. Absorption peaks of the samples can be seen in Table 2.

Encapsulation efficiency of the MEL loaded particles calculated as 73.39%. The Higuchi model had indicated that drug dissolution in varied, modified polymeric release dosage forms [32]. The melatonin was encapsulated PCL displayed a R^2 value of 0.992 and the n value of Korsmeyer-Peppas model is 0.58265. This indicated that the mechanism was non-Fickian Diffusion [33]. In addition, drug-loading rate of the particles could increase by using more MEL in the manufacturing stage of the particles.

It has known that scaffold properties play an essential role in cell growth and morphology and have a direct effect on intracellular interactions. Cellular adhesion, proliferation, and spreading are important factors in cell-scaffold interaction, which effects further differentiation and mineralization [34]. Cellular proliferation is important

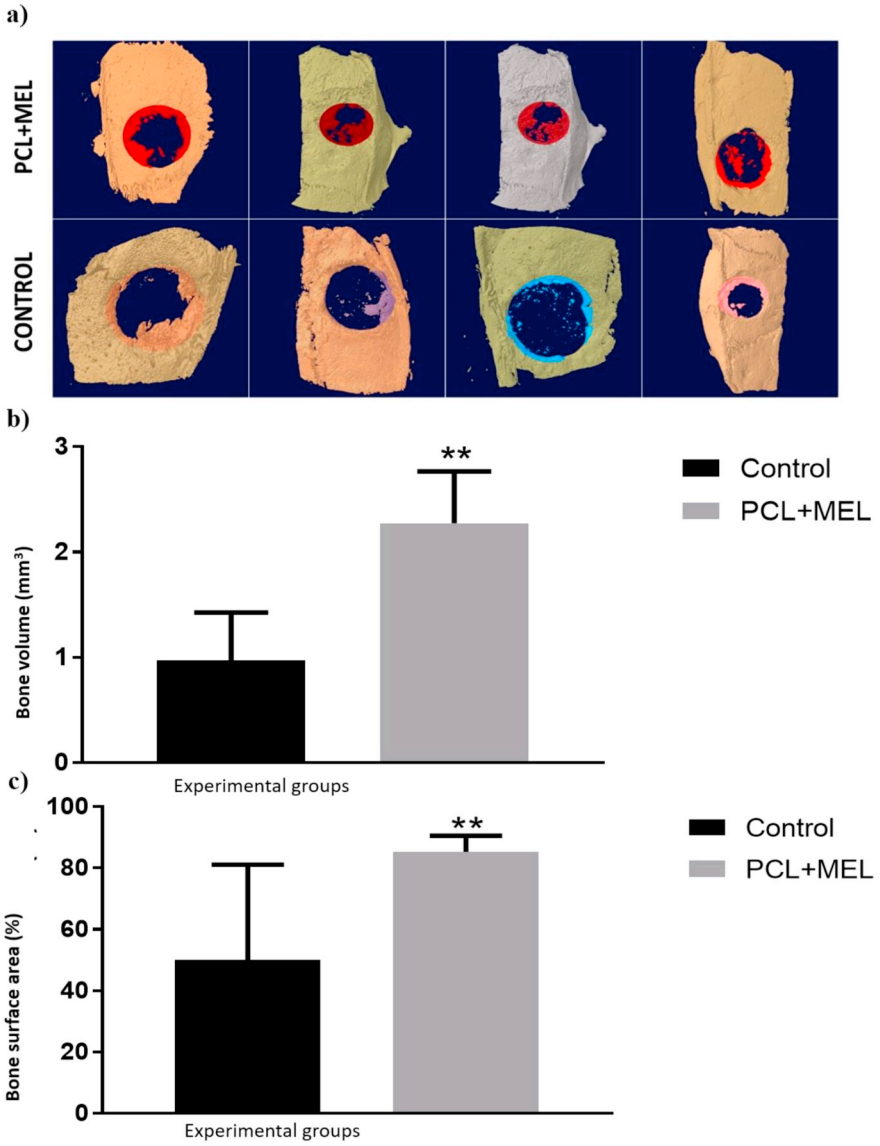


Fig. 8. Representative images, bone volume and distribution of bone surface area/total surface area of experimental groups. (a) Representative Micro-CT images of experimental groups. Treatment groups include empty defects (control); defects treated with 3 wt% PCL + MEL, (b) bone volume of experimental groups. Data are expressed as mean ± SEM; $n = 6/8$ rats/group; $^{**}P < 0.05$, (c) Distribution of bone surface area/total surface area of experimental groups. Data are expressed as mean ± SEM; $n = 6/8$ rats/group; $^{**}P < 0.05$.

Table 1
Processing parameters for fabrication of PCL microparticles.

PCL concentration (wt %)	PCL solution flow rate (ml/h)	Voltage applied (kV)	Fabrication distance (cm)
1	0.5	10	8
3	0.5	10	8
5	1.0	12	8
7	1.5	15	8

for bone healing and melatonin has known to stimulate proliferation of those cells such as human osteoblast, bone cell 3T3L1 and pre-adipocytes [35–39]. Hejazi and Mirzadeh had fabricated 2D PCL scaffolds and 3D nanofiber-microparticle blended PCL (NF/MP PCL) scaffolds with electrospinning and electrospraying and viability of MG-63 cell line was estimated at the day 3, 5, 7, 14, and 21 days and concluded that NF/MP PCL scaffolds had improved cell proliferation, attachment and spreading [40]. Kim et al. had developed polycaprolactone/poly (lactic-co-glycolic acid) (PCL/PLGA), heparin-conjugated and heparin-dopamine conjugated PCL/PLGA scaffolds for controlled release of bone morphogenic protein-2 (BMP-2) (BMP2/Hep/PCL/PLGA), (BMP-′/Hep-DOPA/PCL/PLGA). *In vitro* cell proliferation tests were performed with MG-63 (human osteosarcoma) cells at the days 1, 3, and 7 and all samples had shown over 95% increase but the highest viability was observed for BMP-2/Hep–DOPA/PCL/PLGA at the day 7 [41]. In another study was performed by Gupta et al. biocompatibility of poly (-L-lactic acid)-poly(ε-capro-lactone), gelatine and hydroxyapatite scaffolds (PLACL, PLACL/Gel, PLACL/Gel/HA(blend), PLACL/Gel/HA (sprayed) and TCP) designed by electrospinning and electrospraying technique are tested with hFOB (human fetal osteoblastic) cell line for 5, 10, and 15 days [42]. The significant increase in viability is observed at day 10 and 15 for the blend. At the day 15 of the sprayed scaffolds 78% and 89% viability increase is observed for PLACL/Gel/HA blend and sprayed ones while 52% and 41% increase is observed for PLACL and PLACL/Gel samples. Zhang et al. encapsulated melatonin into poly (lactic-co-glycolic acid) (PLGA) microspheres and release of melatonin [39]. Effect of microspheres on biocompatibility (*in vitro* at the days 1, 3 and 6) and osteogenesis were investigated with human mesenchymal

Table 2
Typical infrared bands of PCL [25].

Position (cm^{-1})	Vibrator	Abbreviation
2949	Symmetric CH_2 stretching	$\nu_{as}(CH_2)$ [26]
2865	Symmetric CH_2 stretching	$\nu_{s}(CH_2)$ [27]
1727	Carbonyl stretching	ν(C=O) [28]
1293	C−O and C−C stretching in the crystalline phase	ν_{cr} [29]
1240	Asymmetric COC stretching	ν_{as}(COC) [30]
1190	OC−O stretching	ν(OC−O) [31]
1170	Symmetric COC stretching	ν_{s}(COC) [25]
1157	C−O and C−C stretching in the amorphous phase	ν_{am} [25]

stem cells (hMSCs) in. 40% release of melatonin in 3 days was followed by slow release for 25 days. PLGA-Mel microspheres had showed no apparent effect on hMSCs proliferation but increased osteoblast differentiation and ALP activity were indicated.

In the light of *in-vitro* cell viability and fluorescent microscopy results electrosprayed scaffolds were found biocompatible. Furthermore, electrosprayed PCL and PCL + MEL scaffolds had shown the time-dependent cellular increase. 2.45% and 7.04% and it could be concluded that melatonin had increased cellular proliferation better than PCL. Fluorescent microscopy images and biocompatibility results also concluded, that cellular proliferation and adhesion on this scaffolds were higher than those of PCL.

Among the different graft materials, autologous bone grafts were considered as best materials due to their combinations of osteoconductive, osteoinductive and osteogenic properties [43–45]. On the other hand, the necessity of secondary surgery causes discomfort of the patient. Furthermore, in large defects, an extra-oral donor site is required [46]. Another important feature associated with the use of extra-oral bones could be their resorption at the recipient site in addition to general anesthesia and hospitalization [47,48]. In addition to these disadvantages of autologous grafts, increasing cost of natural-origin grafts reveals the need for cheaper and effective graft materials. In the present data, it demonstrated the first time encapsulated melatonin hormone was build up in PCL microparticles. Previous studies had indicated, that melatonin has potential benefits in bone remodelling [49–51]. In parallel with present study findings, melatonin had showed wider and longer cortical bones than collagenized porcine bone in a study [52]. Also, in a recent clinical investigation, immediate implants were augmented with autogenous bone graft/melatonin composite graft showed a significant gain in bone density compared with autogenous bone graft alone [53]. Therefore, further investigations are required to appraise the co-application of PCL and melatonin as a graft material.

An ideal graft material should have osteoconductive, osteogenic and osteoinductive properties in addition to biomechanical stability and degradation within an appropriate time [54]. According to the present study data, melatonin encapsulated PCL indicated biomechanical stability and not degraded in four weeks. Additionally, the osteoconductive properties of melatonin were shown in different studies [55,56]. Similar to those findings, in present study, it was demonstrated wide distribution of new bone *in vivo* and proliferation of cells *in vitro* on the material surface. Therefore, further investigations are required to appraise the co-application of PCL and melatonin as a graft material.

5. Conclusion

In this study, melatonin successfully encapsulated in biodegradable PCL microparticles by using electrospraying. Average of 2.30 μm PCL microparticles holds together with nanofibers successfully produced in this study. The FTIR and UV spectrum characterization tests indicated that melatonin could be released 73.39% in 8 h. *In vitro* and *in vivo* findings suggest that encapsulated melatonin in PCL supports bone remodelling. Thus, that encapsulation of melatonin in the polymer with electrospray method is very promising for new synthetic graft material.

Acknowledgments

This study funded by the Marmara University with the BAPKO project (FEN-C-YLP-120417-0177). In addition, authors are grateful to Mr. Hasan EKEER at the Erciyes University Faculty of Dentistry Research Center for his support on the micro-CT measurements and Mr. Deniz Uçar for technical support in the name of Evo Implants, Turkey.

Conflict of interest

The authors declare no conflict of interest.

References

[1] P. Kumar, B. Vinitha, G. Fathima, Bone grafts in dentistry, J. Pharm. Bioallied. 5 (Suppl. 1) (2013) S125.
[2] N. Bock, M.A. Woodruff, D.W. Hutmacher, T.R. Dargaville, Electrospraying, a reproducible method for production of polymeric microspheres for biomedical applications, Polymers 3 (1) (2011) 131–149.
[3] M. Ye, S. Kim, K. Park, Issues in long-term protein delivery using biodegradable microparticles, J. Control. Release 146 (2) (2010) 241–260.
[4] M. Zamani, M.P. Prabhakaran, S. Ramakrishna, Advances in drug delivery via electrospun and electrosprayed nanomaterials, Int. J. Nanomedicine 8 (2013) 2997.
[5] Y. Wu, S.J. Kennedy, R.L. Clark, Polymeric particle formation through electrospraying at low atmospheric pressure, J Biomed Mater Res B Appl Biomater 90 (1) (2009) 381–387.
[6] S. Chakraborty S, I.C. Liao, A. Adler, K.W. Leong, Electrohydrodynamics: a facile technique to fabricate drug delivery systems, Adv. Drug Deliv. Rev. 61 (12) (2009) 1043–1054.
[7] D.X. Tan, L.C. Manchester, R. Hardeland, S. Lopez-Burillo, J.C. Mayo, R.M. Sainz, R.J. Reiter, Melatonin: a hormone, a tissue factor, an autocoid, a paracoid, and an antioxidant vitamin, J. Pineal Res. 34 (1) (2003) 75–78.
[8] Z. Ostrowska, B. Kos-Kudla, B. Marek, D. Kajdaniuk, P. Staszewicz, B. Szapska, J. Strzelczyk, The influence of pinealectomy and melatonin administration on the dynamic pattern of biochemical markers of bone metabolism in experimental osteoporosis in the rat, Neuro. Endocrinol. Lett. 23 (2002) 104–109.
[9] S. Shafei, J. Foroughi, L. Stevens, C.S. Wong, O. Zabihi, M. Naebe, Electroactive nanostructured scaffold produced by controlled deposition of PPy on electrospun PCL, Res. Chem. Intermed. 43 (2) (2017) 1235–1251.
[10] Y. Hong, Y. Li, Y. Yin, D. Li, G. Zou, Electrohydrodynamic atomization of quasi-monodisperse drug-loaded spherical/wrinkled microparticles, J. Aerosol Sci. 39 (6) (2008) 525–536.
[11] V.R. Sinha, K. Bansal, R. Kaushik, R. Kumria, A. Trehan, Poly-ε-caprolactone microspheres and nanospheres: an overview, Int. J. Pharm. 278 (1) (2004) 1–23.
[12] M.A. Woodruff, D.W. Hutmacher, The return of a forgotten polymer—polycaprolactone in the 21st century, Adv. Polym. Sci. 35 (10) (2010) 1217–1256.
[13] J. Xie, J.C. Marijnissen, C.H. Wang, Microparticles developed by electrohydrodynamic atomization for the local delivery of anticancer drug to treat C6 glioma in vitro, Biomaterials 27 (17) (2006) 3321–3332.
[14] S. Gun, M. Edirisinghe, E. Stride, Encapsulation of superparamagnetic iron oxide nanoparticles in poly-(lactide-co-glycolic acid) microspheres for biomedical applications, Mater. Sci. Eng. C Mater. Biol. Appl. 33 (6) (2013) 3129–3137.
[15] Y. Wu, S.J. Kennedy, R.I. Clark, Polymeric particle formation through electrospraying at low atmospheric pressure, J Biomed Mater Res B Appl Biomater 90 (1) (2009) 381–387.
[16] O. Barou, D. Valentin, L. Vico, C. Tirode, A. Barbier, C. Alexandre, M.H. Lafage-Proust, High-resolution three-dimensional micro-computed tomography detects bone loss and changes in trabecular architecture early: comparison with DEXA and bone histomorphometry in a rat model of disuse osteoporosis, Investig. Radiol. 37 (1) (2002) 40–46.
[17] M. Rasekh, Z. Ahmad, R. Cross, J. Hernandez-Gil J, J.D. Wilton-Ely, P.W. Miller, Facile preparation of drug-loaded tristearin encapsulated superparamagnetic iron oxide nanoparticles using coaxial electrospray processing, Mol. Pharm. 14(6) (2017) 2010–2023.
[18] Y. Wu, S.J. Kennedy, R.L. Clark, Polymeric particle formation through electrospraying at low atmospheric pressure, J Biomed Mater Res B Appl Biomater 90 (1) (2009) 381–387.
[19] Y.K. Hwang, U. Jeong, E.C. Cho, Production of uniform-sized polymer core-shell microcapsules by coaxial electrospraying, Langmuir 24 (6) (2008) 2446–2451.
[20] F.L. Zhou, P.L. Hubbard Cristinacce, S.J. Eichhorn, G.J. Parker, Preparation and characterization of polycaprolactone microspheres by electrospraying, Aerosol Sci. Technol. 50 (11) (2016) 1201–1215.
[21] A. Polini, D. Pisignano, M. Parodi, R. Quarto, S. Scaglione, Osteoinduction of human mesenchymal stem cells by bioactive composite scaffolds without supplemental osteogenic growth factors, PLoS One 6 (10) (2011) e2621.

[22] J.C. Reichert, M.E. Wullschleger, A. Cipitria, J. Lienau, T.K. Cheng, M.A. Schütz, G.N. Duda, U. Nöth, J. Eulert, D.W. Hutmacher, Custom-made composite scaffolds for segmental defect repair in long bones, Int. Orthop. 35 (8) (2011) 1229–1236.
[23] M. Sabzichi, N. Samadi, J. Mohammadian, H. Hamishehkar, M. Akbarzadeh, O. Molavi, Sustained release of melatonin: a novel approach in elevating efficacy of tamoxifen in breast cancer treatment, Colloids Surf. B Biointerfaces 145 (2016) 64–71.
[24] S. Pajoumshariati, S.K. Yavari, M.A. Shokrgozar, Physical and biological modification of polycaprolactone electrospun nanofiber by panax ginseng extract for bone tissue engineering application, Ann. Biomed. Eng. 44 (5) (2016) 1808–1820.
[25] T. Elzein, M. Nasser-Eddine, C. Delaite, S. Bistac, P. Dumas, FTIR study of polycaprolactone chain organization at interfaces, J. Colloid Interface Sci. 273 (2) (2004) 381–387.
[26] S.N. Gorodzha, M.A. Surmeneva, R.A. Surmenev, Fabrication and characterization of polycaprolactone cross-linked and highly-aligned 3-D artificial scaffolds for bone tissue regeneration via electrospinning technology, IOP Conf, Ser. Mater. Sci. Eng. 98 (1) (2015) 012024.
[27] S.N. Gorodzha, M.A. Surmeneva, R.A. Surmenev, Fabrication and characterization of polycaprolactone cross-linked and highly-aligned 3-D artificial scaffolds for bone tissue regeneration via electrospinning technology, IOP Conf. Ser.: Mater. Sci. Eng. 98 (2015) 012024.
[28] D. Walsh, T. Furuzono, J. Tanaka, Preparation of porous composite implant materials by in situ polymerization of porous apatite containing ε-caprolactone or methyl methacrylate, Biomaterials 22 (11) (2001) 1205–1212.
[29] T. Elzein, H. Awada, M. Nasser-Eddine, C. Delaite, M. Brogly, A model of chain folding in polycaprolactone-b-polymethyl methacrylate diblock copolymers, Thin Solid Films 483 (1) (2005) 388–395.
[30] M. Ibrahim, A. Nada, D.E. Kamal, Density functional theory and FTIR spectroscopic study of carboxyl group, Indian J. Pure Ap. Phy. 43 (2005) 911–917.
[31] T. Elzein, M. Nasser-Eddine, C. Delaite, S. Bistac, P. Dumas, FTIR study of polycaprolactone chain organization at interfaces, J. Colloid. Intertace Sci. 273 (2) (2004) 381–387.
[32] R.W. Korsmeyer, R. Gurny, E. Doelker, P. Buri, N.A. Peppas, Mechanisms of solute release from porous hydrophilic polymers, Int. J. Pharm. 15 (1) (1983) 25–35.
[33] V.A.D. Mello, E. Ricci-Júnior, Encapsulation of naproxen in nanostructured system: structural characterization and in vitro release studies, Química Nova 34 (6) (2011) 933–939.
[34] J.R. Venugopal, S. Low, A.T. Choon, A.B. Kumar, S. Ramakrishna, Nanobioengineered electrospun composite nanofibers and osteoblasts for bone regeneration, Artif. Organs 32 (5) (2008) 388–397.
[35] J.A. Roth, B.G. Kim, W.L. Lin, M.I. Cho, Melatonin promotes osteoblast differentiation and bone formation, J. Biol. Chem. 274 (31) (1999) 22041–22047.
[36] O. Nakade, H. Koyama, H. Ariji, A. Yajima, T. Kaku, Melatonin stimulates proliferation and type I collagen synthesis in human bone cells in vitro, J. Pineal Res. 27 (2) (1999) 106–110.
[37] K. Satomura, S. Tobiume, R. Tokuyama, Y. Yamasaki, K. Kudoh, E. Maeda, M. Nagayama, Melatonin at pharmacological doses enhances human osteoblastic differentiation in vitro and promotes mouse cortical bone formation in vivo, J. Pineal Res. 42 (3) (2007) 231–239.
[38] K. Zwirska-Korczala, J. Jochem, M. Adamczyk-Sowa, P. Sowa, R. Polaniak, E. Birkner, M. Latocha, K. Pılc, R. Suchanek, Influence of melatonin on cell proliferation, antioxidative enzyme activities and lipid peroxidation in 3T3-L1 preadipocytes-an in vitro study, J. Physiol. Pjarmacol 56 (2005) 91–99.
[39] L. Zhang, J. Zhang, Y. Ling, C. Chen, A. Liang, Y. Peng, H. Chang, P. Su, D. Huang, Sustained release of melatonin from poly (lactic-co-glycolic acid)(PLGA) microspheres to induce osteogenesis of human mesenchymal stem cells in vitro, J. Pineal Res. 54 (1) (2013) 24–32.
[40] F. Hejazi, H. Mirzadeh, Novel 3D scaffold with enhanced physical and cell response properties for bone tissue regeneration, fabricated by patterned electrospinning/electrospraying, J. Mater. Sci. Mater. Med. 27 (9) (2016) 143.
[41] T.H. Kim, Y.P. Yun, Y.E. Park, S.H. Lee, W. Yong, J. Kundu, W.J. Jung, J.H. Shim, D.W. Cho, H.R. Song, In vitro and in vivo evaluation of bone formation using solid freeform fabrication-based bone morphogenic protein-2 releasing PCL/PLGA scaffolds, Biomed. Mater. 9 (2) (2014) 025008.
[42] D. Gupta, J. Venugopal, S. Mitra, V.G. Dev, S. Ramakrishna, Nanostructured biocomposite substrates by electrospinning and electrospraying for the mineralization of osteoblasts, Biomaterials 30 (11) (2009) 2085–2094.
[43] P. Galindo-Moreno, G. Avila, J.E. Fernández-Barbero, F. Mesa, F. O'Valle-Ravassa, H.L. Wang, Clinical and histologic comparison of two different composite grafts for sinus augmentation: a pilot clinical trial, Clin. Oral Implants Res. 19 (2008) 755–759.
[44] M. Chiapasco, M. Zaniboni, L. Rimondini, Autogenous onlay bone grafts vs. alveolar distraction osteogenesis for the correction of vertically deficient edentulous ridges: a 2–4-year prospective study on humans, Clin. Oral Implants Res. 18 (2007) 432–440.
[45] O. Moses, C.E. Nemcovsky, Y. Langer, H. Tal, Severely resorbed mandible treated with iliac crest autogenous bone graft and dental implants: 17-year follow-up, Int. J. Oral Maxillofac. Implants 22 (2007) 1017–1021.
[46] C. Zizelmann, R. Schoen, M.C. Metzger, R. Schmelzeisen, A. Schramm, B. Dott, K.H. Bormann, N.C. Gellrich, Bone formation after sinus augmentation with engineered bone, Clin. Oral Implants Res. 18 (1) (2007) 69–73.
[47] A.L. Zétola, T. Verbicaro, S. Littieri, R. Larson, A.F. Giovanini, T.M. Deliberador, Recombinant human bone morphogenetic protein type 2 in the reconstruction of atrophic maxilla: case report with long-term follow-up, J, Indian Soc. Periodontol 18 (2014) 781–785.
[48] D. Schwartz-Arad, S. Dori, Intraoral autogenous onlay block bone grafting for implant dentistry, Refuat Hapeh Vehashinayim 19 (2002) 35–39.
[49] D.P. Cardinali, M.G. Ladizesky, V. Boggio, R.A. Curteta, C. Mautalen, Melatonin effects on bone: experimental facts and clinical perspectives, J. Pineal Res. 34 (2) (2003) 81–87.
[50] M.G. Ladizesky, V. Boggio, L.E. Albornoz, P.O. Castrillon, C. Mautalen, D.P. Cardinali, Melatonin increases oestradiol-induced bone formation in ovariectomized rats, J. Pineal Res. 34 (2003) 143–151.
[51] S. Maria, P.A. Witt-Enderby, Melatonin effects on bone: potential use for the prevention and treatment for osteopenia, osteoporosis, and periodontal disease and for use in bone-grafting procedures, J. Pineal Res. 56 (2014) 15–125.
[52] J.L. Calvo-Guirado, M.P. Ramírez-Fernández, G. Gomez-Moreno, J.E. Mate-Sanchez, R. Delgado-Ruiz, J. Guardia, L. Lopez-Mari, A. Barone, A.J. Ortiz-Ruiz, J.M. Martinez-Gonzalez, L.A. Bravo, Melatonin stimulates the growth of new bone around implants in the tibia of rabbits, J. Pineal Res. 49 (2010) 356–363.
[53] H.H.A. Hazzaa, N.Sh. El-Kilani, S.A. Elsayed, P.M. Abd El Massieh, Evaluation of immediate implants augmented with autogenous bone/melatonin composite graft in the esthetic zone: a randomized controlled trial, J. Prosthodont. 0 (2017) 1–6.
[54] P.V. Giannoudis, J.J. Chris Arts, G. Schmidmaier, S. Larsson, What should be the characteristics of the ideal bone graft substitute? Injury 42 (2011) S1–S2.
[55] F. Luchetti, B. Canonico, D. Bartolini, M. Arcangeletti, S. Ciffolilli, G. Murdolo, M. Prioddi, S. Papa, R.J. Reiter, F. Galli, Melatonin regulates mesenchymal stem cell differentiation: a review, J. Pineal Res. 56 (4) (2014) 382–397.
[56] H. Shino, A. Hasuike, Y. Arai, M. Honda, K. Isokawa, S. Sato, Melatonin enhances vertical bone augmentation in rat calvaria secluded spaces, Med. Oral Patol. Oral Cir. Bucal. 21 (1) (2016) e122–e126.